Computers, Materials & Continua
DOI: 10.32604/cmc.2023.032940
Article

FPGA Implementation of Extended Kalman Filter for Parameters Estimation of Railway Wheelset

Khakoo Mal[1,2,*], Tayab Din Memon[1,3], Imtiaz Hussain Kalwar[4] and Bhawani Shankar Chowdhry[5]

[1]Department of Electronic Engineering, Mehran University of Engineering & Technology, Jamshoro, 76062, Pakistan
[2]Sukkur IBA University, Sukkur, 65200, Pakistan
[3]Design and Creative Technology, Torrens University Australia, 196 Flinders Street, Melbourne, 3000, VIC, Australia
[4]Department of Electronics and Power Engineering, Pakistan Navy Engineering College NUST, Karachi, 75350, Pakistan
[5]NCRA-Condition Monitoring Systems Lab, Mehran University of Engineering & Technology, Jamshoro, 76062, Pakistan
*Corresponding Author: Khakoo Mal. Email: khakoo.mal@iba-suk.edu.pk
Received: 02 June 2022; Accepted: 09 August 2022

Abstract: It is necessary to know the status of adhesion conditions between wheel and rail for efficient accelerating and decelerating of railroad vehicle. The proper estimation of adhesion conditions and their real-time implementation is considered a challenge for scholars. In this paper, the development of simulation model of extended Kalman filter (EKF) in MATLAB/Simulink is presented to estimate various railway wheelset parameters in different contact conditions of track. Due to concurrent in nature, the Xilinx® System-on-Chip Zynq Field Programmable Gate Array (FPGA) device is chosen to check the onboard estimation of wheel-rail interaction parameters by using the National Instruments (NI) myRIO® development board. The NI myRIO® development board is flexible to deal with nonlinearities, uncertain changes, and fast-changing dynamics in real-time occurring in wheel-rail contact conditions during vehicle operation. The simulated dataset of the railway nonlinear wheelset model is tested on FPGA-based EKF with different track conditions and with accelerating and decelerating operations of the vehicle. The proposed model-based estimation of railway wheelset parameters is synthesized on FPGA and its simulation is carried out for functional verification on FPGA. The obtained simulation results are aligned with the simulation results obtained through MATLAB. To the best of our knowledge, this is the first time study that presents the implementation of a model-based estimation of railway wheelset parameters on FPGA and its functional verification. The functional behavior of the FPGA-based estimator shows that these results are the addition of current knowledge in the field of the railway.

Keywords: Adhesion force; extended kalman filter; FPGA implementation; railway wheelset; real-time estimation; wheel-rail interaction

1 Introduction

From the sustainable development point of view in modern society, the mode of transport that seems to be least harmful to the natural environment is railroad transport because it emits less carbon dioxide, one of the causal agents of global warming as compared to its tonnage capacity than other automobiles [1]. All around the world, a huge railway infrastructure is established and is being spread more due to increased public demand for railway transport. But due to lack of system up-gradation and knowledge of modern condition monitoring systems, the derailment events are being increased which is a great concern. The dynamic performance of the entire rolling stock is controlled by the forces generated between wheel and track [2], therefore the wheel-rail interaction area is a very important part of rolling stock. Adhesion force is the transmitted tangential force between wheel and rail [3,4].

Therefore, it is necessary to estimate the contact forces and depending parameters. In [5,6], a model-based method using EKF is offered to estimate the nonlinear forces between wheel and rail interaction. However, the approach is not tested on all track conditions. In [7], data-driven technique using particle swarm optimization (PSO) and kernel extreme learning machine (KELM) is presented for identification of adhesion between wheel and track of heavy-haul locomotive. However, the technique is only tested in normal adhesion condition, hence more research is required for estimation of adhesion state in low adhesion conditions. Traction force is estimated in [8,9] by applying Kalman filter to develop slip controller. However, the algorithm is not tested on all adhesion conditions. In [10], adhesion conditions between wheels and rails are estimated by designing an observer for the development of advanced braking control system. But the track irregularities and weather conditions were not considered during the investigation. The comparison between theoretical and measured creep curves is performed in [11] to estimate the impact on creep forces in wheel-rail interaction. However, the creep curves for different types of contaminated rails not clear enough, so systematic work on the influence of creep curves for all conditions is required. A lot of research is being carried out for the estimation of wheel-track contact conditions mainly scholars use model-based techniques [12–15].

Many techniques are found during the literature review for accurate estimation of railway wheel-rail contact conditions. But, no appropriate evidence is found for the implementation of estimation scheme for wheelset parameter. In [16], the implementation of EKF on FPGA for state of charge (SOC) estimation of a lithium-ion battery is presented. The sensor fusion for omnidirectional mechatronic system using EKF is developed in [17] to estimate the position and orientation. The experimental results are obtained on myRIO-1900 through LabVIEW. A system is developed in [18] to construct variable-order fractional chaotic systems using LabVIEW for its implementation on the Xilinx FPGA chip through myRIO-1900. But, EKF implementation on FPGA for wheel-rail contact conditions has not been reported in the literature yet.

Therefore, in this paper, we extend the work reported in [19,20], by the implementation of the extended Kalman filter algorithm on FPGA for estimation of different wheelset parameters by taking all adhesion conditions and both vehicle operation modes of traction and braking. However, the implementation of EKF on FPGA for the estimations needs several iterative matrix operations which are very computationally expensive [21]. In meeting these requirements, the computer-based National Instruments myRIO® development platform is selected. It uses some high-throughput arithmetic functions, an Advanced extensible Interface (AXI-4 Stream interface), and handshaking protocol to manage the computation effectively and efficiently [22]. The novelty of this work is to present the

- implementation of the extended Kalman filter based model estimator for railway wheelset parameters estimation and its hardware synthesize in Xilinx System-on-Chip Zynq FPGA device using NI myRIO® platform and computation of the chip-area utilization.

- comparison of the MATLAB and FPGA simulation results for functional verification of railway parameter estimations in dry, wet, greasy, and extremely slippery as well as switching of track conditions from normal to very slippery conditions and vice versa.

The rest of the paper is organized as follows. The estimator design is described in Section 2, while in Section 3 EKF implementation on FPGA is presented. In Section 4, FPGA results are shown and the conclusion and future work is discussed in Section 5.

2 Estimator Design for Railway Wheelset Parameters

Many research scholars used model-based estimation techniques by applying simple Kalman filter to estimate the parameters of railway wheelset [2,8,9,23,24]. But, a single Kalman filter, due to the nonlinear behavior of railway dynamics, is not suitable for wheel-track interaction system. Therefore, a model-based approach using EKF is used to estimate wheelset parameters. The EKF does linearization in current mean and covariance by evaluating Jacobian matrices and their partial derivatives. The block diagram of EKF with wheelset model is shown in Fig. 1.

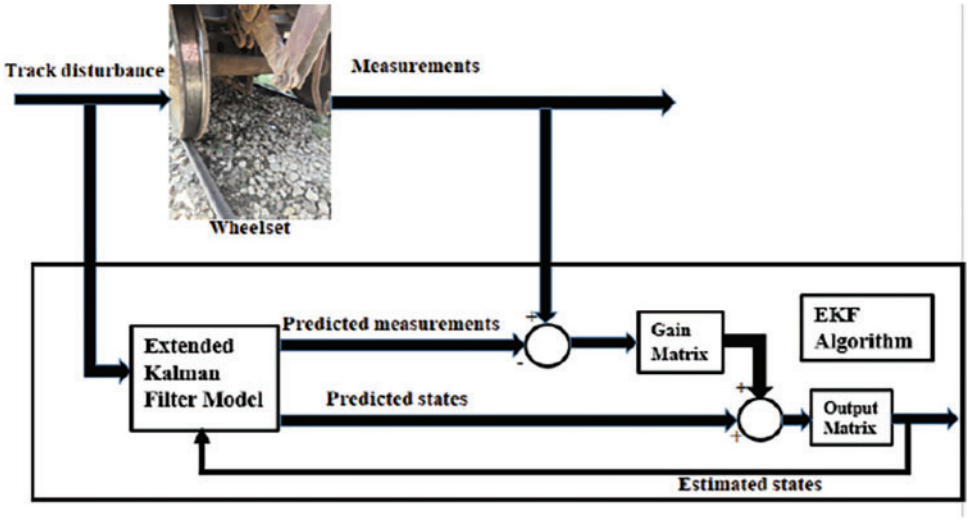

Figure 1: Block diagram of EKF and wheelset model

The EKF algorithm is developed by using the nonlinear wheelset model available in [20]. By using lateral and yaw motion equations of railway wheelset, Eq. (1) is furnished for the development of EKF.

$$\begin{bmatrix} \dot{y} \\ \dot{\Psi} \\ \ddot{y} \\ \ddot{\Psi} \end{bmatrix} = \begin{bmatrix} 0 & 0 & 1 & 0 \\ 0 & 0 & 0 & 1 \\ 0 & \frac{2}{m_w}\frac{F_a}{\gamma} & -\frac{2}{m_w v}\frac{F_a}{\gamma} & 0 \\ -\frac{2L_g\lambda_w}{I_w r_0}\frac{F_a}{\gamma} & -\frac{k_w}{I_w} & 0 & -\frac{2L_g^{\,2}}{I_w v}\frac{F_a}{\gamma} \end{bmatrix} \begin{bmatrix} y \\ \Psi \\ \dot{y} \\ \dot{\Psi} \end{bmatrix} + \begin{bmatrix} 0 \\ 0 \\ 0 \\ \frac{2L_g}{I_w r_0}\frac{F_a}{\gamma} \end{bmatrix} y_t \tag{1}$$

The key purpose of this section is to design a novel scheme to identify the variations in wheel-track interaction conditions, so yaw and lateral dynamics are enough to identify these variations. Hence, longitudinal dynamics are ignored in Eq. (1).

The first step of the EKF algorithm is time update or prediction and the second step is measurement update or correct [25] as shown in Fig. 2.

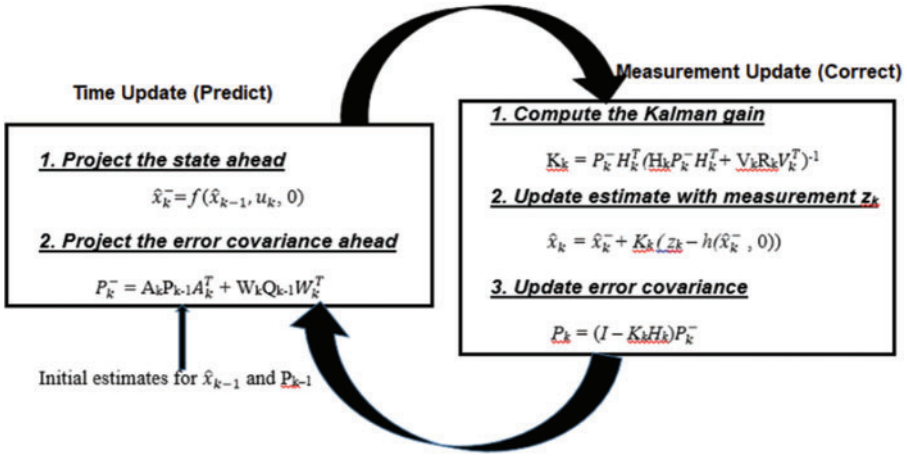

Figure 2: A complete picture of the operation of the extended Kalman filter

where f and h are nonlinear functions concerning the states of process and measurement respectively, and $A_k = \frac{\partial f}{\partial x} | \hat{x}_k,\ u_k,\ k$ and $H_k = \frac{\partial h}{\partial x} | \hat{x}_k,\ u_k,\ k$. Further, Tab. 1 gives detail about the terms used in the EKF algorithm.

Table 1: Terms used in the EKF algorithm

Symbol	Description
$\hat{x}_k^-$	Discretized a-priori estimated process
x_k	Discretized a-postriori estimated process
$\hat{P}_k^-$	A-priori estimate error of process covariance
P_k	An estimate error of measurement covariance
F_k	Jacobian matrix of process matrix
H_k	Jacobian matrix of measurement matrix
Q_k	Noise covariance of process matrix
R_k	Noise covariance of measurement matrix
K_k	Kalman gain
$\tilde{m}_k$	Measured output

To make the state matrix $\boldsymbol{x}$ of the EKF algorithm, the variables given in (2) e.g., velocity in lateral direction ($\dot{y}$), yaw rate ($\dot{\Psi}$), slip ratio (γ), friction coefficient (μ), and adhesion force (F_a) are taken and for measurement matrix $\boldsymbol{m}$, the variables e.g., lateral acceleration and yaw rate are used [20].

$$\boldsymbol{x} = \begin{bmatrix} \dot{y} & \dot{\Psi} & \gamma & \mu & F_a \end{bmatrix}^T, \boldsymbol{m} = \begin{bmatrix} \ddot{y} & \dot{\Psi} \end{bmatrix}^T \tag{2}$$

The process variables used in (2) are continuous being driven from the nonlinear wheelset model, however, the EKF algorithm is discrete, so by using the Forward Euler method, these continuous

variables are discretized [26] as in Eqs. (3) to (7) [20].

$$\dot{y}_k = \dot{y}_{k-1} + \frac{2\tau}{m_w}\left(\Psi\frac{F_{ak-1}}{\gamma_{k-1}} - \frac{\dot{y}_{k-1}}{v}\frac{F_{ak-1}}{\gamma_{k-1}}\right) \tag{3}$$

$$\dot{\Psi}_k = \dot{\Psi}_{k-1} + \frac{\tau}{I_w}\left(\frac{2y_t L_g}{r_0}\frac{F_{ak-1}}{\gamma_{k-1}} - \frac{2yL_g\lambda_w}{r_0}\frac{F_{ak-1}}{\gamma_{k-1}} - \frac{2\dot{\Psi}_{k-1}L_g^{\,2}}{v}\frac{F_{ak-1}}{\gamma_{k-1}} - K_w\Psi\right) \tag{4}$$

$$\gamma_k = \sqrt{\left(\frac{L_g\dot{\Psi}_{k-1}}{v} + \frac{\lambda_w(y - y_t)}{r_0}\right)^2 + \left(\frac{\dot{y}_{k-1}}{v} - \Psi\right)^2} \tag{5}$$

$$\mu_k = u_0[(1-A)\ e^{(-B\gamma_{k-1}v)} + A] \tag{6}$$

$$F_{ak} = \frac{2N\mu_{k-1}}{\pi}\left[\frac{k_A\frac{2}{3}\frac{a^2bc}{N\mu_{k-1}}\gamma_{k-1}}{1+\left(k_A\frac{2}{3}\frac{a^2bc}{N\mu_{k-1}}\gamma_{k-1}\right)^2} + \arctan\left(k_S\frac{2}{3}\frac{a^2bc}{N\mu_{k-1}}\gamma_{k-1}\right)\right] \tag{7}$$

The Jacobian matrix of process matrix $x_k = \begin{bmatrix}\dot{y}_k\\ \dot{\Psi}_k\\ \gamma_k\\ \mu_k\\ F_{ak}\end{bmatrix}$ is

$$A_k == \begin{bmatrix}
\frac{\partial f1(x)_k}{\partial y'_k} & \frac{\partial f1(x)_k}{\partial \Psi'_k} & \frac{\partial f1(x)_k}{\partial \gamma_k} & \frac{\partial f1(x)_k}{\partial U_k} & \frac{\partial f1(x)_k}{\partial F_k}\\
\frac{\partial f2(x)_k}{\partial y'_k} & \frac{\partial f2(x)_k}{\partial \Psi'_k} & \frac{\partial f2(x)_k}{\partial \gamma_k} & \frac{\partial f2(x)_k}{\partial U_k} & \frac{\partial f2(x)_k}{\partial F_k}\\
\frac{\partial f3(x)_k}{\partial y'_k} & \frac{\partial f3(x)_k}{\partial \Psi'_k} & \frac{\partial f3(x)_k}{\partial \gamma_k} & \frac{\partial f3(x)_k}{\partial U_k} & \frac{\partial f3(x)_k}{\partial F_k}\\
\frac{\partial f4(x)_k}{\partial y'_k} & \frac{\partial f4(x)_k}{\partial \Psi'_k} & \frac{\partial f4(x)_k}{\partial \gamma_k} & \frac{\partial f4(x)_k}{\partial U_k} & \frac{\partial f4(x)_k}{\partial F_k}\\
\frac{\partial f5(x)_k}{\partial y'_k} & \frac{\partial f5(x)_k}{\partial \Psi'_k} & \frac{\partial f5(x)_k}{\partial \gamma_k} & \frac{\partial f5(x)_k}{\partial U_k} & \frac{\partial f5(x)_k}{\partial F_k}
\end{bmatrix} \tag{8}$$

And the Jacobian matrix of the measurement matrix $m_k = \begin{bmatrix}\ddot{y}_k\\ \dot{\Psi}_k\end{bmatrix}$ is [19]

$$H_k = \begin{bmatrix}
\frac{\partial h1(m)_k}{\partial y'_k} & \frac{\partial h1(m)_k}{\partial \Psi'_k} & \frac{\partial h1(m)_k}{\partial \gamma_k} & \frac{\partial h1(m)_k}{\partial U_k} & \frac{\partial h1(m)_k}{\partial F_k}\\
\frac{\partial h2(m)_k}{\partial y'_k} & \frac{\partial h2(m)_k}{\partial \Psi'_k} & \frac{\partial h2(m)_k}{\partial \gamma_k} & \frac{\partial h2(m)_k}{\partial U_k} & \frac{\partial h2(m)_k}{\partial F_k}
\end{bmatrix} \tag{9}$$

The detail of the parameters used in the EKF design for wheelset parameter estimation is shown in Tab. 2.

Table 2: Variables used in EKF design for wheelset parameter estimation [20]

No.	Notation	Description	Value
1	γ	Slip ratio	
2	r_0	Radius of wheel	0.5 meter
3	L_g	Track half gauge	0.75 meter
4	λ_w	Wheel conicity	0.15 rad
5	V	Longitudinal velocity of vehicle	
6	Y	Motion in lateral direction	meter
7	y_t	Rail irregularities in lateral direction	meter
8	Ψ	Yaw angle	radians
9	F_a	Adhesion force	
10	I_w	Yaw moment of inertia of wheelset	700 kgm^2
11	K_w	Yaw stiffness	5×10^6 N//rad
12	m_w	Wheel weight with induction motor	1250 kg
13	τ	Forward Euler discretizing step size	
14	u_0	Highest friction coefficient at no slip velocity	
15	A	Friction coefficient ratio at infinity slip velocity to u_0	
16	B	Coefficient of exponential friction decrease	
17	N	Normal force	
18	k_A	Reduction factor around adhesion	
19	k_S	Reduction factor in a slip	
20	a, b	Half-axes of contact ellipse	
21	c	Coefficient of contact shear stiffness	

The offered estimation approach illustrated in Fig. 1 is designed in Simulink for simulation [26]. MATLAB Function tool of Simulink version 9.1 is used to develop and verify the EKF algorithm with 50 microseconds fixed step size. The initial velocity in forward direction is set at 5 m/s and the vehicle is operated in accelerating and decelerating modes. For exciting lateral dynamics, an input of random track disturbance having ±8 mm amplitude is applied to the model in lateral direction.

Simulations in five different adhesion conditions are carried out for 25 s in traction mode and for 25 s in braking mode of the vehicle. The EKF is found a valid estimation technique for all adhesion conditions to estimate wheelset parameters in both operation modes of accelerating and decelerating. During simulation, the strength of the algorithm is also tested in the switching of track conditions from normal to very slippery and vice-versa. Therefore, the proposed model can now be implemented on FPGA for condition monitoring of rolling stock.

3 FPGA Implementation of EKF

The main objective of this research is to create a novel model-based method to identify variations in wheel-rail interaction conditions with real-time implementation on FPGA. The Block diagram of the complete proposed model is shown in Fig. 3. As this research work comprising on simulation through MATLAB and its implementation on FPGA. The first part of the proposed model is a railway

wheelset modeled in MATLAB available in [20]. The second part is the EKF algorithm designed in MATLAB and described in Section 2, while the last part of the proposed model is explained in this section.

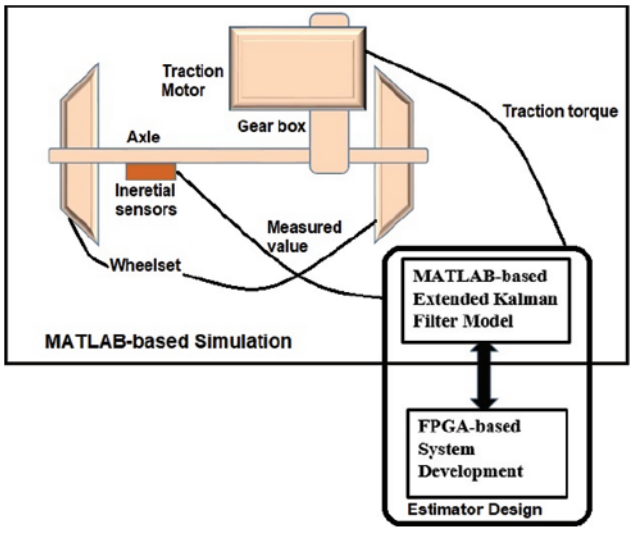

Figure 3: Block diagram of the complete proposed model

The EKF designed for railway wheelset parameter estimation is implemented on myRIO Zynq FPGA through LabVIEW [17,18]. The National Instruments myRIO® is a computer-based real-time embedded evaluation board developed with a dual core Advanced RISC Machine (ARM) processor and an Artix-7 FPGA chip incorporating onboard memory and have a Universal Serial Bus (USB) port to connect host Personal Computer (PC) [22]. It requires LabVIEW software a system-design platform and a development environment from National Instruments. The overall system partitioning of myRIO and system portioning in FPGA device are illustrated in Fig. 4. The functional block diagram of Fig. 5 shows the operation flow in myRIO. The dataset of the wheelset model extracted from MATLAB is saved on Solid state drives (SSD) which is read by the Real time (RT) using File Input/output (I/O). The dataset is parsed and streamed to FPGA using DMA-FIFO (AXI-4 Stream interface).

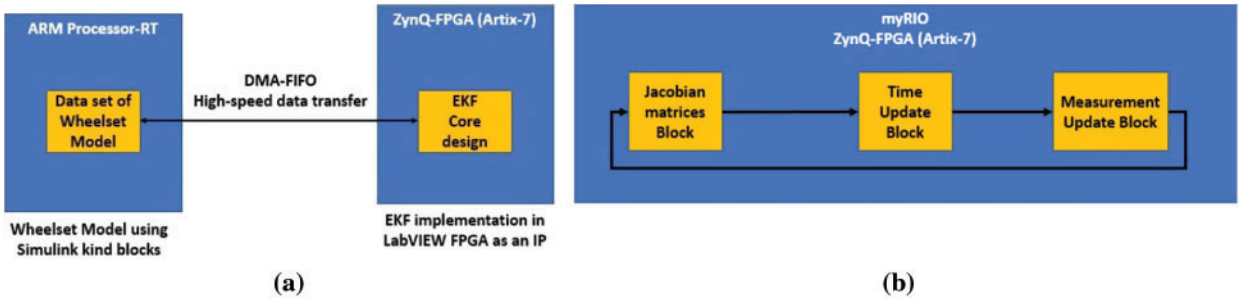

Figure 4: (a) System partitioning of myRIO and (b) System partitioning in Zynq-FPGA device

The FPGA has 04 main cores i.e., internal calculation, process Jacobian matrix, measurement Jacobian matrix, and time/measurement update. To optimize resource utilization, each core uses shared multiplication blocks using arbiter. After the synthesize of the proposed model as shown in Fig. 5 the chip-area utilization on the Zynq FPGA device is given in Tab. 3.

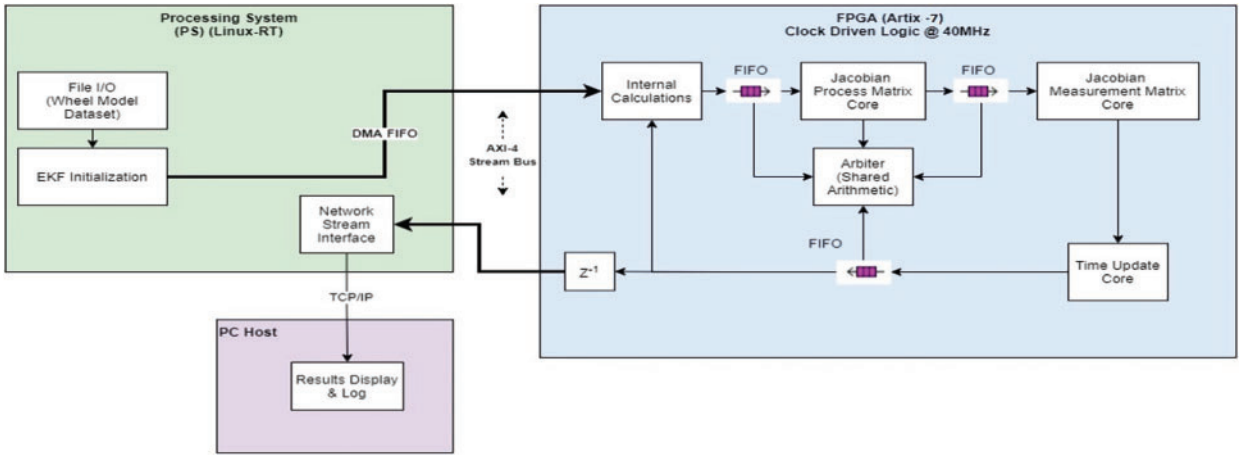

Figure 5: Functional flow diagram of myRIO

Table 3: Resource utilization

Resource	Available	Used	Utilization (%)
Total slices	4400	4400	100
Slice registers	35200	16315	46.3
Slice LUTs	17600	15902	90.4
Block RAMs	60	43	71.7
DSP48s	80	33	41.2

The explanation of EKF implementation on FPGA through NI myRIO-1900 board is given in Fig. 6.

4 FPGA Results

The functional behavior of FPGA implemented EKF is analyzed in different conditions (e.g., dry, wet, greasy, extremely slippery). The most important wheelset parameters i.e., adhesion coefficient, slip ratio, and yaw rate are investigated because the dynamics of entire railway vehicle depend on these parameters. The FPGA model is also tested when the track condition is changed abruptly from dry to extremely slippery conditions. The traction and braking operation modes of railroad vehicle are used. The step size of the entire system is set at 50 microseconds, which means 1000000 samples in 50 s are implemented on FPGA Zynq device for each scenario. As the Xilinx Zynq chip frequency is 40 MHz, which is much more than the input changes frequency. Furthermore, the complete Simulink model in Fig. 7 illustrates how track conditions change. In Simulink model, Polach parameters [20] for each track conditions are changed through multi-port switches by controlling input feed from stair

generator. Input 1 from stair generator is set for dry condition, inputs 2 for wet, 3 for greasy and 4 for extremely slippery condition are set.

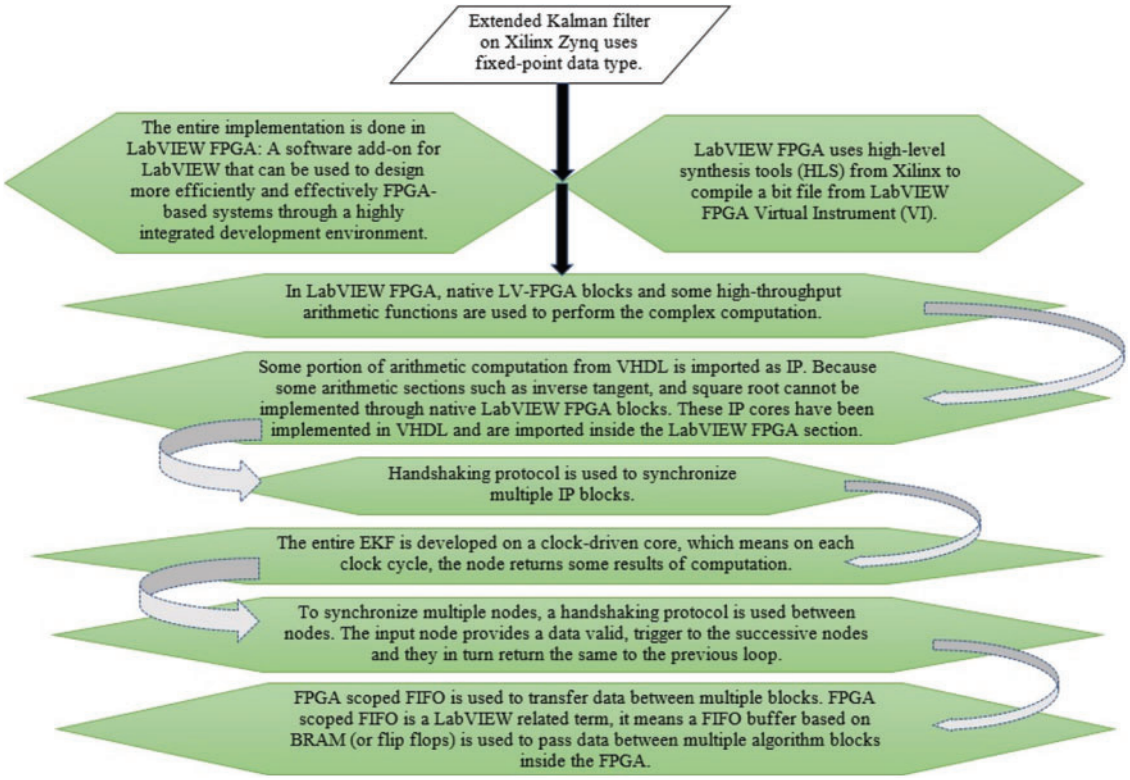

Figure 6: Flowchart explaining EKF implementation on FPGA through NI myRIO

4.1 Dry Condition Implementing Results

The dry track condition or the normal adhesion condition of wheel-rail contact is analyzed in 25 s of traction mode and 25 s of braking mode of the vehicle. In the simulation model of the railway wheelset, the exerted torque and linear velocity of the vehicle are given in Fig. 8.

The functional verification of adhesion coefficient of FPGA-based EKF is done as shown in Fig. 9. FPGA-based EKF response follows the adhesion coefficient of the wheelset model, but the error on sharp transition is comparatively high. However, the root mean square (RMS) of error (0.0401) is small as compared to the RMS of estimated adhesion coefficient (0.3613), which becomes about 11%. FPGA-based EKF estimates the slip ratio, but little error is shown in Fig. 10. Again, the RMS of error (6.4204e-04) is small as compared to the RMS of estimated actual slip ratio (0.0057), which is nearly 11%. The main reason of high errors is possibly due to high rate of velocity. In Fig. 11 yaw rate is estimated successfully by FPGA based estimator, but oscillations are generated because of variation in tractive torque and random rail disturbance in the lateral direction.

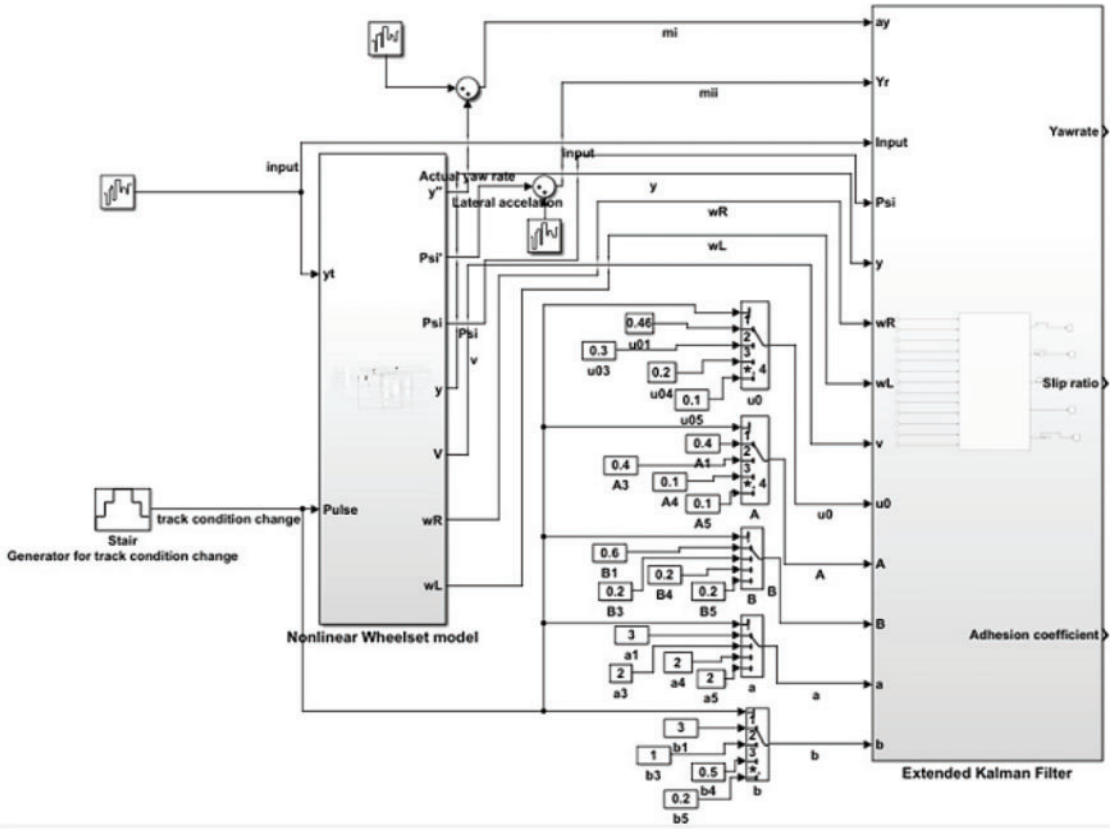

Figure 7: Simulation model for estimation of railway wheelset parameter using EKF

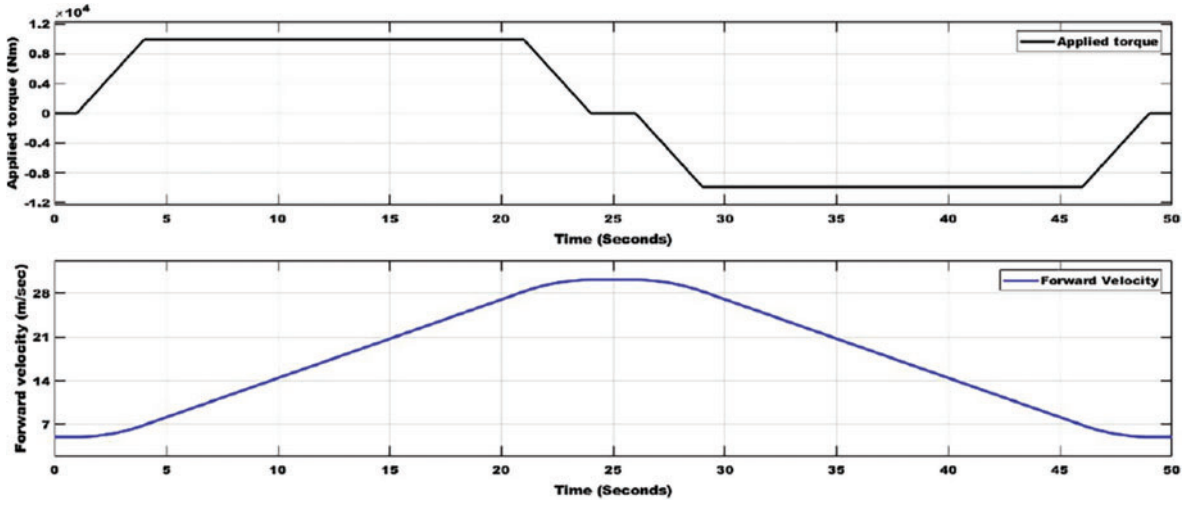

Figure 8: Tractive torque (top) and changing linear velocity (bottom) in normal condition of wheel-track contact

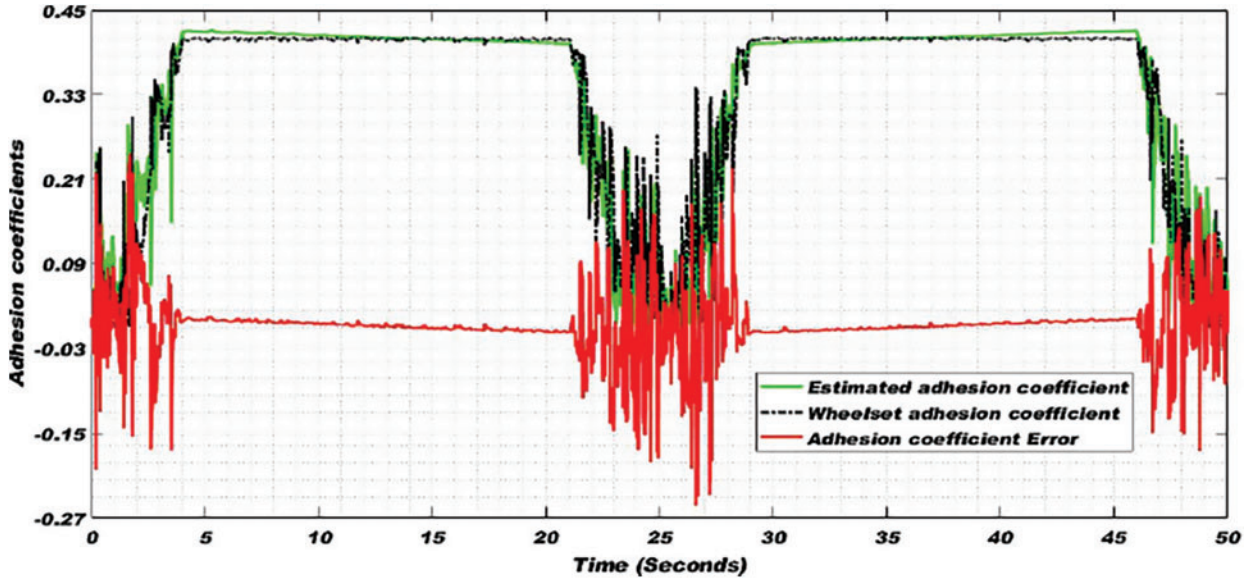

Figure 9: Dry condition adhesion coefficient of FPGA-based EKF in comparison with the adhesion coefficient of wheelset model

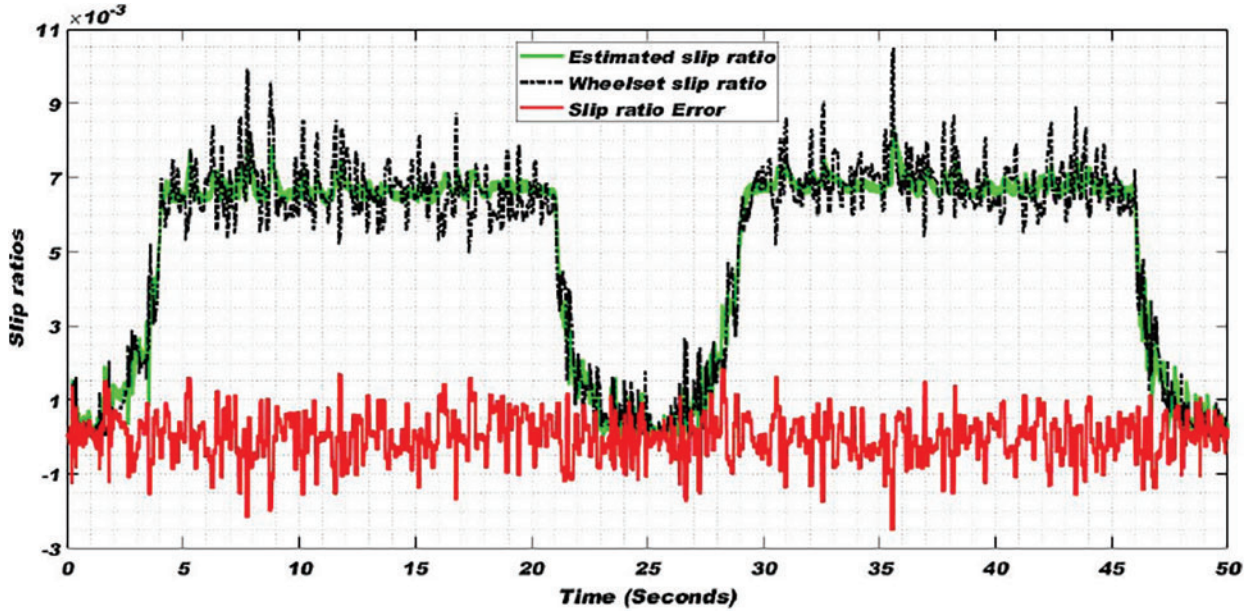

Figure 10: Dry condition slip ratio of FPGA-based EKF in comparison with the slip ratio of wheelset model

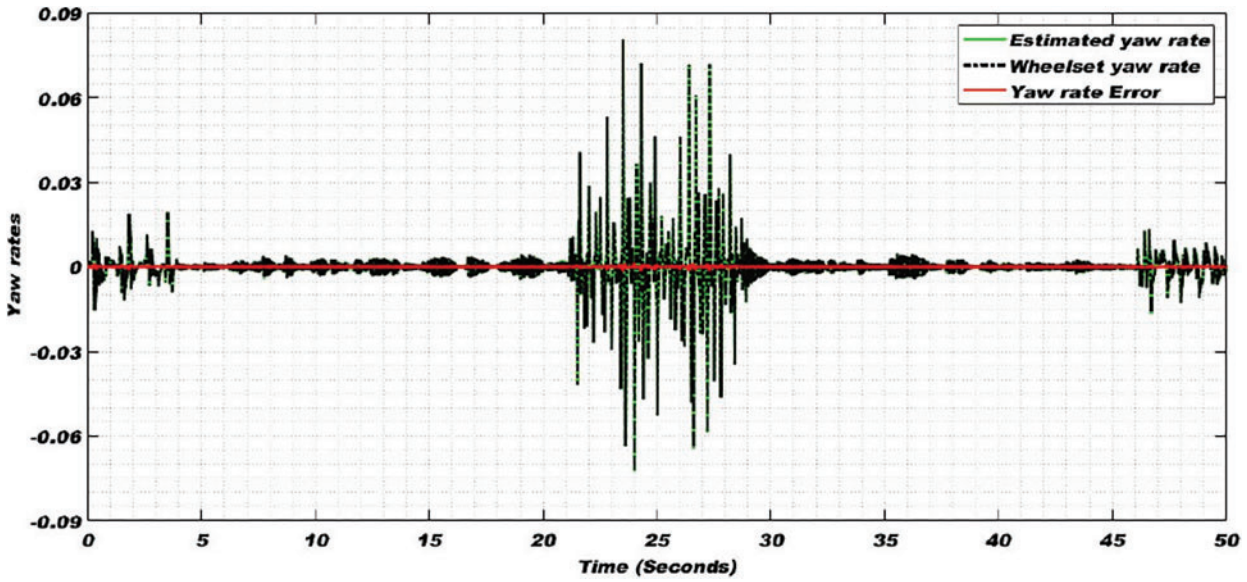

Figure 11: Dry condition yaw rate of FPGA-based EKF in comparison with the yaw ratio of wheelset model

4.2 Wet Condition Implementing Results

Due to dew or light rain on the railway track, the contaminated track becomes wet which decreases adhesion coefficient below that of a dry track [27]. Wet condition estimating parameters of FPGA-based EKF in comparison with simulated wheelset parameters are shown in Fig. 12. The FPGA-based response is found robust in both vehicle operation modes of traction and braking.

4.3 Greasy Condition Implementing Results

Oils on railway tracks due to any reason in minute quantity are found a complex mixture of contaminants and become the reason for adhesion level reduction [28]. The FPGA-based estimator also estimates the adhesion coefficient, slip ratio, and yaw rate in oily track condition for both traction and braking modes as shown in Fig. 13.

4.4 Extremely Slippery Condition Implementing Results

Extremely low adhesion levels between the wheel and rail may be found due to all or some weather conditions, local environmental and industrial conditions (e.g., leaf contamination, snow, rain, oil spills, industrial pollution). In extremely slippery condition, the FPGA-based estimator is also fit for the estimation of adhesion coefficient, slip ratio, and yaw rate as illustrated in Fig. 14.

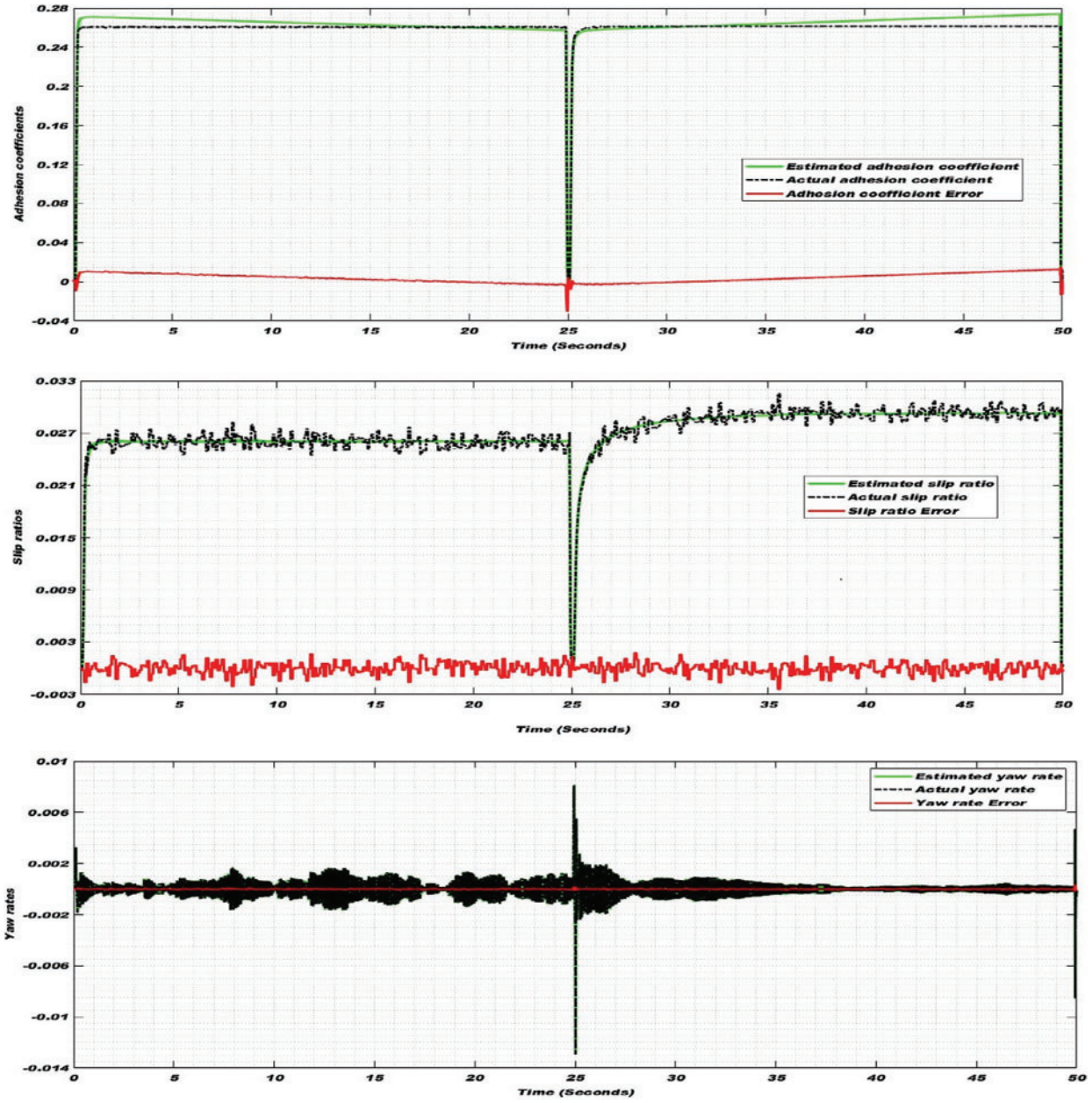

Figure 12: Wet condition adhesion coefficient (top), slip ratio (middle), and yaw rate (bottom) of FPGA-based EKF in comparison with the simulation parameters of the wheelset model

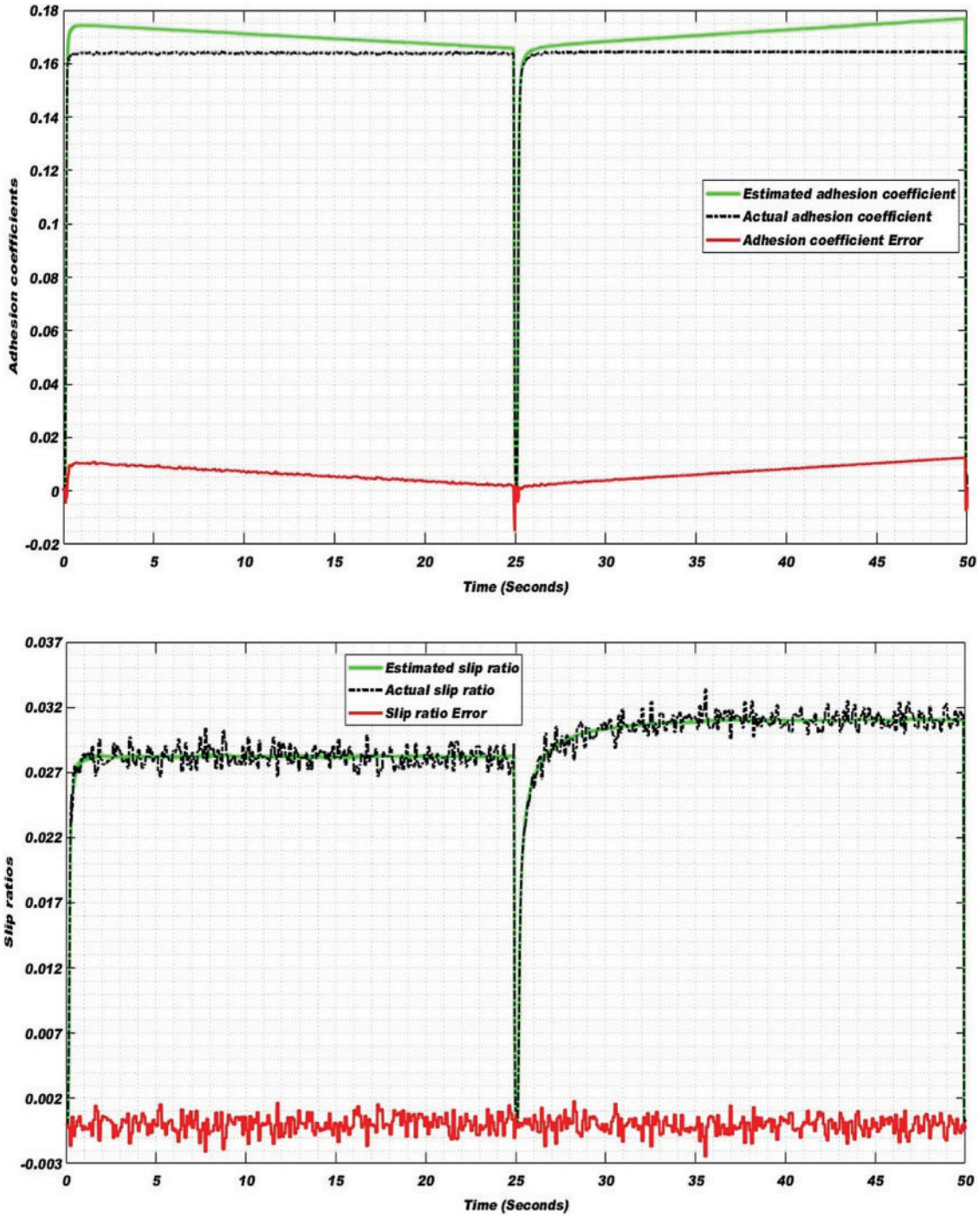

Figure 13: (Continued)

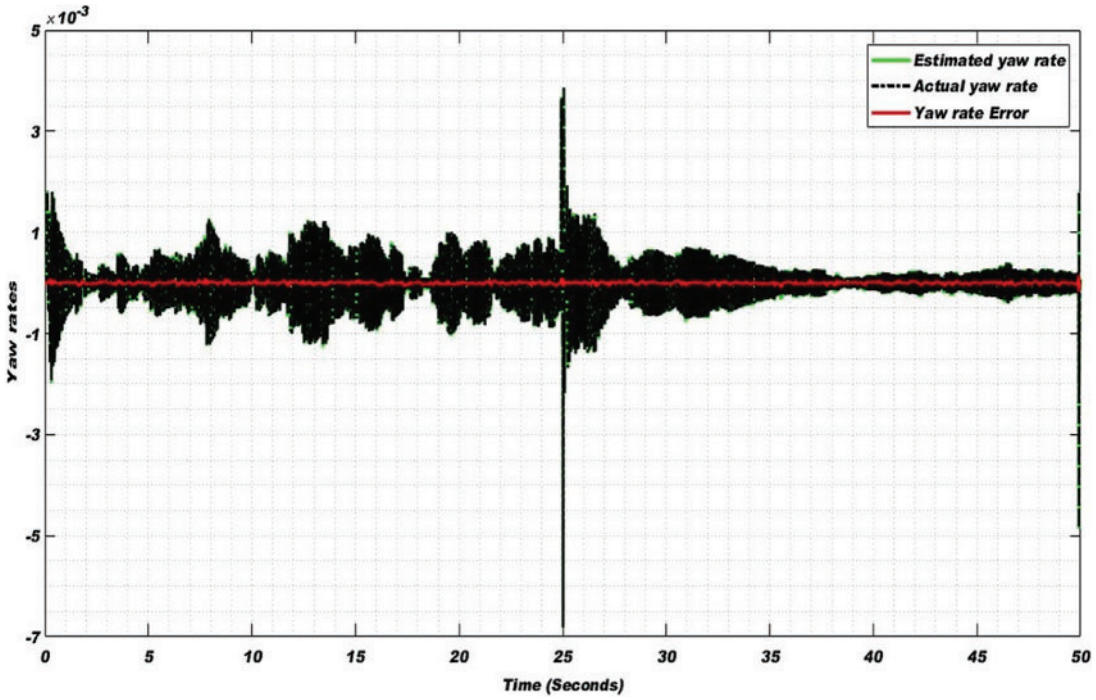

Figure 13: Greasy condition adhesion coefficient (top), slip ratio (middle) and yaw rate (bottom) of FPGA-based EKF in comparison with the simulation parameters of wheelset model

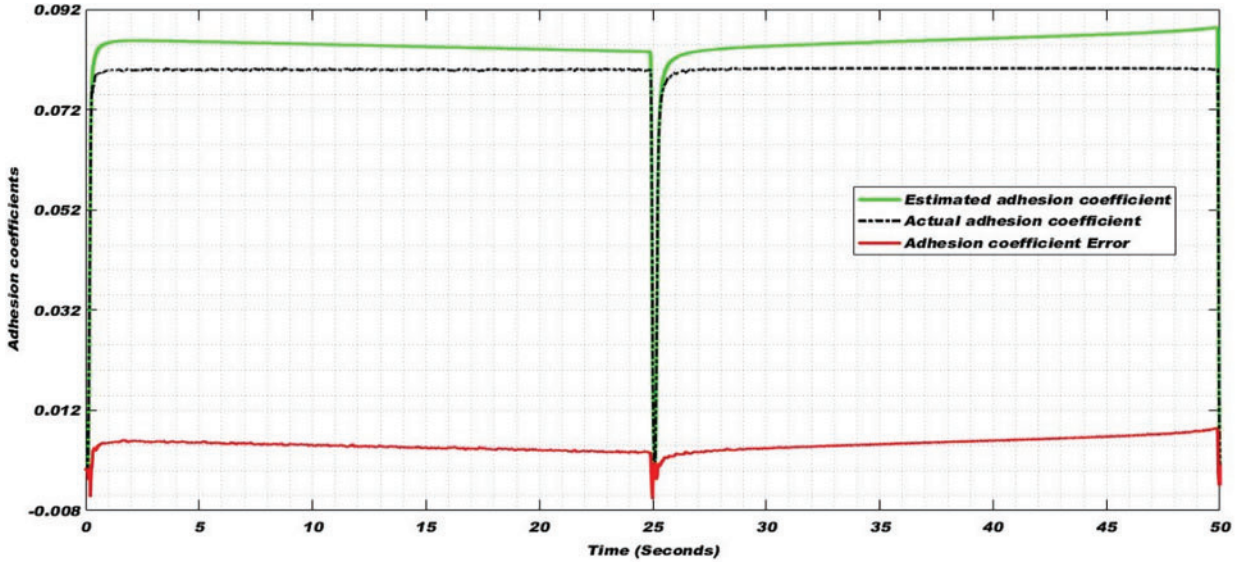

Figure 14: (Continued)

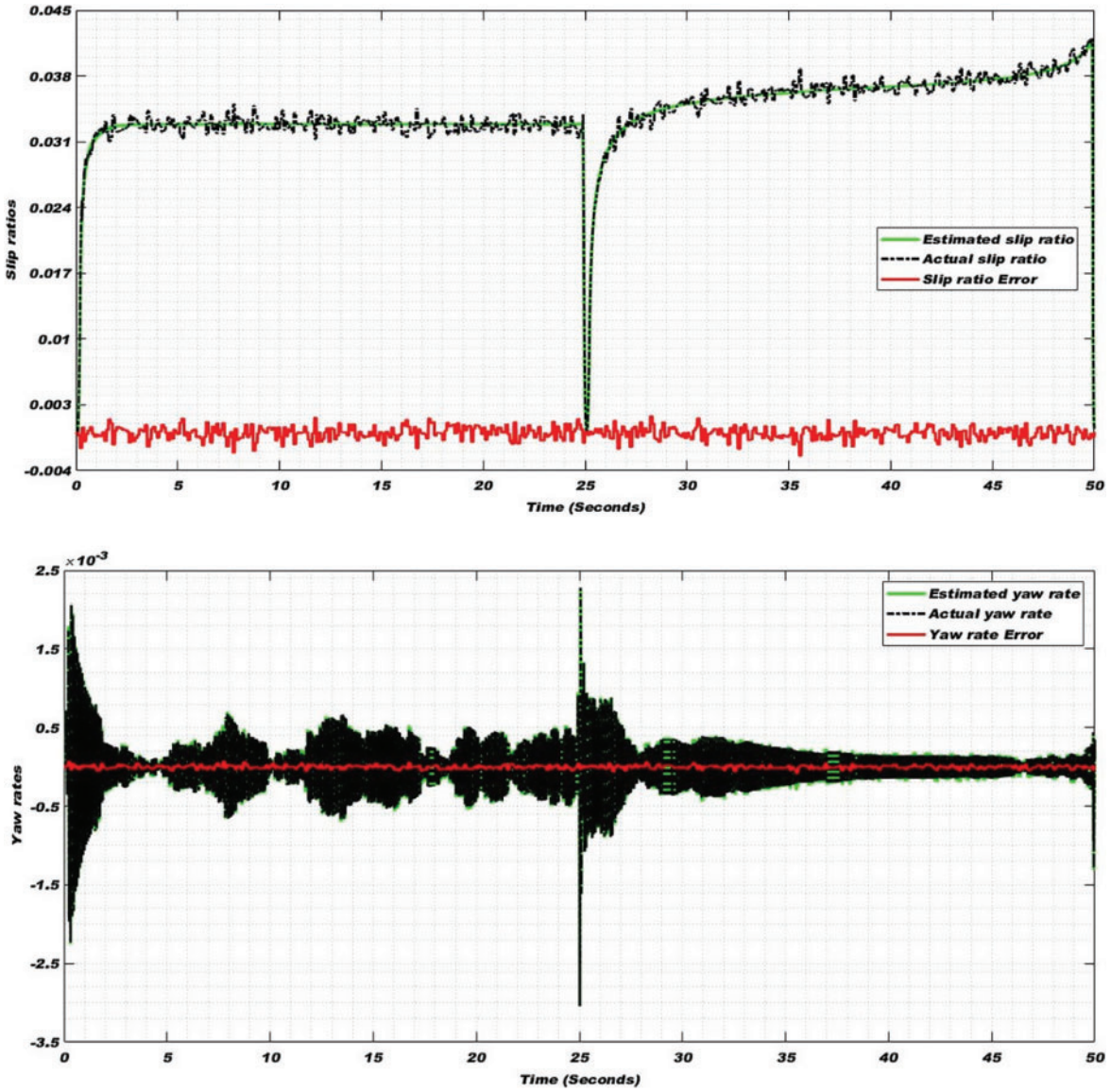

Figure 14: Extremely slippery condition adhesion coefficient (top), slip ratio (middle) and yaw rate (bottom) of FPGA-based EKF in comparison with the simulation parameters of wheelset model

4.5 Switching from Normal to Extremely Slippery Conditions and Vice Versa

FPGA-based EKF response follows the adhesion coefficient of the wheelset model, but the error in starting and ending is comparatively high. Higher error is due to complex scenario i.e., vehicle is operated in operation modes of traction and braking and adhesion condition changes after every 6.25 s from better (dry) condition to worst (extremely slippery) condition as shown in Fig. 15. However, the RMS of error (0.0346) is not high as compared to RMS of estimated adhesion coefficient (0.1885), which becomes about 18%. In the complex scenario, slip ratio and yaw rate of FPGA-based EKF give an excellent performance as shown in Fig. 16.

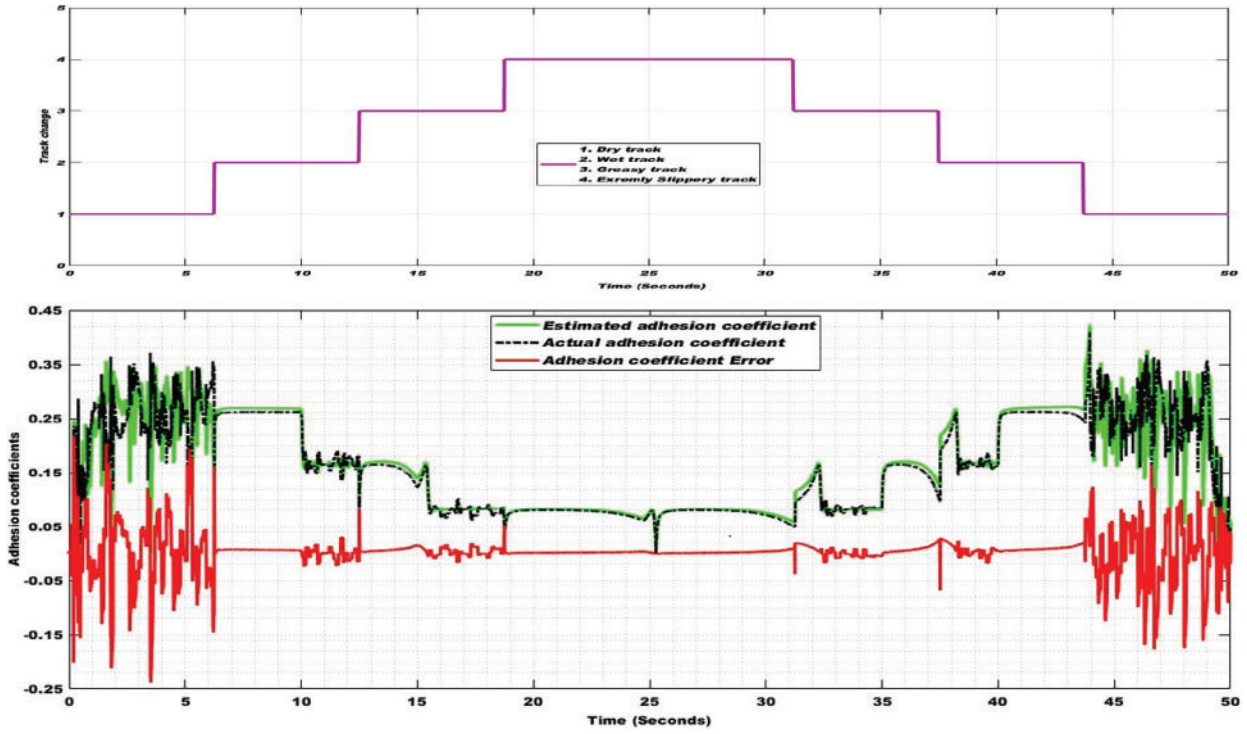

Figure 15: All track conditions adhesion coefficient of FPGA-based EKF in comparison with the adhesion coefficient of wheelset model

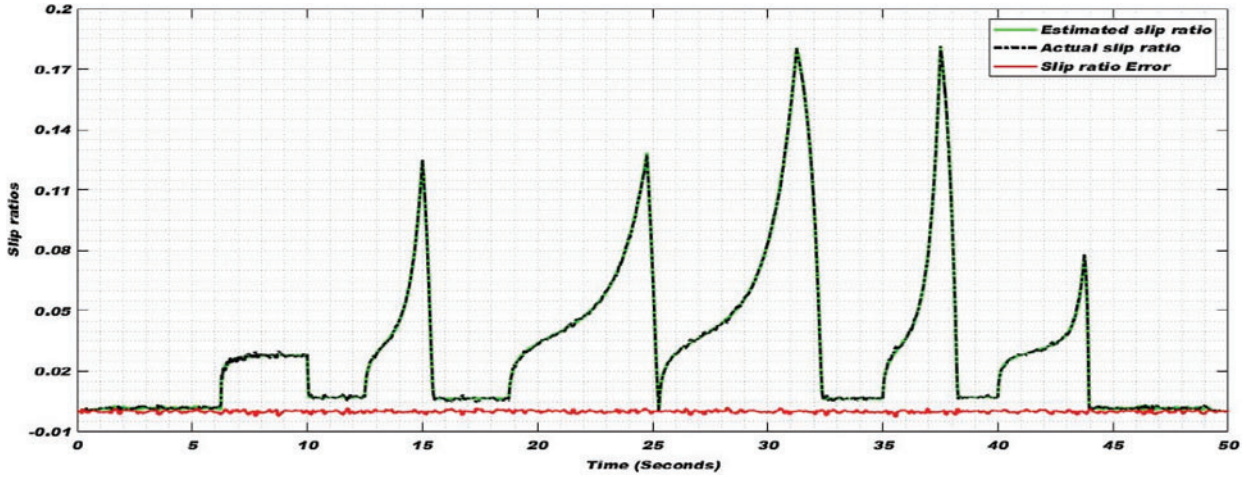

Figure 16: (Continued)

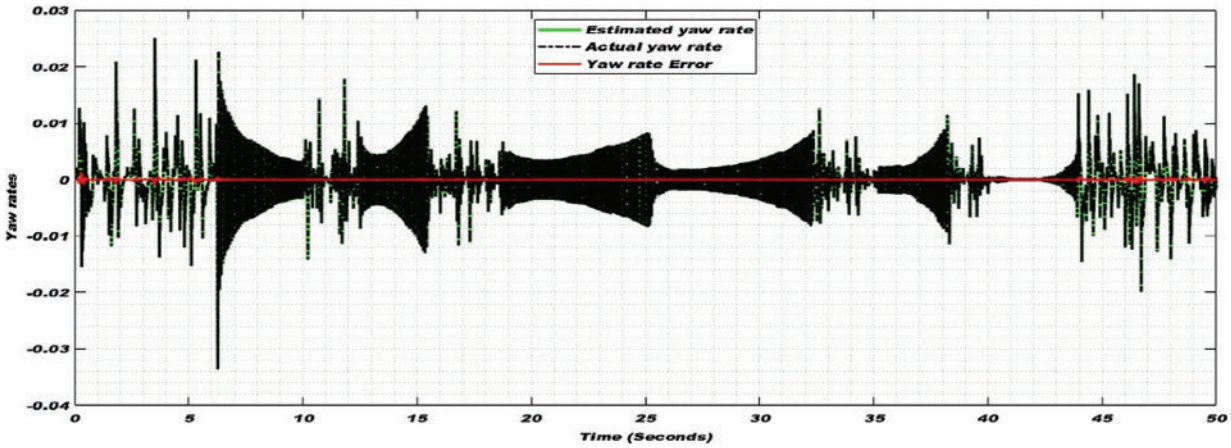

Figure 16: All track conditions slip ratio (top) and yaw rate (bottom) of FPGA-based EKF in comparison with the slip ratio and yaw rate of wheelset model

As shown in Figs. 9 to 16 the FPGA-based EKF is an effective estimation approach to estimate wheelset parameters in operation modes of accelerating and decelerating.

To statistically evaluate the functional behavior of the FPGA-based estimator, the RMSs of estimating error and FPGA-based estimator are calculated with percentage. The RMS calculation with percentage for the estimation of all track conditions is given in Tab. 4.

Table 4: RMS Percentage of estimating error

Track condition	Adhesion coefficient			Slip ratio			Yaw rate (rad/sec)		
	FPGA RMS	*ERROR RMS*	ERROR RMS (%AGE)	*FPGA RMS*	*ERROR RMS*	ERROR RMS (%AGE)	*FPGA RMS*	*ERROR RMS*	ERROR RMS (%AGE)
Dry	0.3613	0.0401	11.09	0.0057	6.4204e-04	11.26	0.0061	6.8146e-05	1.123
Wet	0.2637	0.006	2.284	0.0272	6.6920e-04	2.462	6.5462e-04	2.3712e-05	3.622
Greasy	0.1699	0.0073	4.297	0.0292	6.6963e-04	2.296	4.6208e-04	2.2914e-05	4.958
Extremely Slippery	0.0847	0.0053	6.23	0.0343	6.7020e-04	1.954	2.9909e-04	2.2486e-05	7.518
Track Transition	0.1885	0.0346	18.35	0.048	6.6382e-04	1.383	0.0038	4.9813e-05	1.306

It can be seen that the percentages of error RMS validate the efficiency of the estimator. Therefore, implementation and functionally verification of extended Kalman filter on FPGA is a novel contribution to railway and these results are a value-addition to the current knowledge available in the literature.

5 Conclusion and Future Work

In this paper, an estimator based on EKF is designed in Simulink to estimate nonlinear wheelset parameters. Then it is implemented on FPGA Xilinx Zynq chip built-in on computer-based national

instrument board myRIO by using LabVIEW software. The functional verification of the FPGA-based estimator is done by analyzing different wheelset parameters effectively in all adhesion conditions. The FPGA estimator not only demonstrated robust results at the constant velocity of railroad vehicle on a dry track but equally showed excellent results in operation modes of accelerating and decelerating in wet, oily, and very slippery track conditions. The strength of EKF developed in FPGA is also tested in the switching of track conditions from normal to very slippery conditions and vice-versa during vehicle operation. The FPGA-based extended Kalman filter is also evaluated and validated statistically by calculating the RMSs of estimating error and the response of FPGA synthesized estimator. These results confirm that the nonlinear wheelset parameters estimator is realizable onboard with state-of-the-art system-on-chip small devices. To the best of our knowledge, implementation of the extended Kalman filter based estimator and its functional verification on FPGA is the very first time reported. These results are a new addition to the existing knowledge of railway condition monitoring systems approaches.

However, FPGA chip resource utilization is considerably high. Point to the future is to possibly do modifications in existing design to improve the performance in terms of reducing the estimating error and resource utilization. More work is required to obtain the optimum solution for Area-Performance-Power analysis of FPGA devices by adding constraint or selecting developing an Application Specific Integrated Chip.

Acknowledgement: The authors would like to acknowledge the "National Center of Robotics and Automation (NCRA) Condition Monitoring Systems Laboratory", part of the NCRA project of Higher Education Commission Pakistan at Mehran University of Engineering and Technology, Jamshoro, for supporting this work and Sukkur IBA University management for financial support to one of us (Khakoo Mal).

Funding Statement: This research work is fully supported by the NCRA project of Higher Education Communication Pakistan.

Conflicts of Interest: The authors declare that they have no conflicts of interest to report regarding the present study.

References

[1] A. C. Mariusz Kostrzewski, "Rail vehicle and rail track monitoring system–a key part in transport sustainable development," *The Wroclaw School of Banking Research Journal*, vol. 15, no. 1, pp. 59–74, 2014.

[2] I. Hussain, T. X. Mei and R. T. Ritchings, "Estimation of wheel-rail contact conditions and adhesion using the multiple model approach," *Vehicle System Dynamics*, vol. 51, no. 1, pp. 32–53, 2013.

[3] S. Shrestha, Q. Wu and M. Spiryagin, "Review of adhesion estimation approaches for rail vehicles," *International Journal of Rail Transportation*, vol. 7, no. 2, pp. 79–102, 2019.

[4] Y. Q. Sun, C. Cole and M. Spiryagin, "Monitoring vertical wheel-rail contact forces based on freight wagon inverse modelling," *Advances in Mechanical Engineering*, vol. 7, no. 5, pp. 1–11, 2015.

[5] S. Strano and M. Terzo, "On the real-time estimation of the wheel-rail contact force by means of a new nonlinear estimator design model," *Mechanical Systems and Signal Processing*, vol. 105, pp. 391–403, 2018.

[6] Y. Zhao and B. Liang, "Re-adhesion control for a railway single wheelset test rig based on the behaviour of the traction motor," *Vehicle System Dynamics*, vol. 51, no. 8, pp. 1173–1185, 2013.

[7] J. Liu, L. Liu, J. He, C. Zhang and K. Zhao, "Wheel/rail adhesion state identification of heavy-haul locomotive based on particle swarm optimization and kernel extreme learning machine," *Journal of Advanced Transportation*, vol. 2020, pp. 1–6, 2020.

[8] T. Ishrat, "Slip control for trains using induction motor drive," Ph.D. Thesis, Queensland University of Technology, 2020.
[9] P. D. Hubbard, C. Ward, R. Dixon and R. Goodall, "Verification of model-based adhesion estimation in the wheel-rail interface," *Chemical Engineering Transactions*, vol. 33, pp. 757–762, 2013.
[10] S. Shrestha, "Estimation of adhesion conditions between wheels and rails for the development of advanced braking control system," Ph.D. Thesis, Central Queensland University, 2021.
[11] I. Persson, M. Spiryagin and C. Casanueva, "Influence of non-dry condition creep curves in switch negotiation," *Vehicle System Dynamics*, vol. 2022, pp. 1–13, 2022.
[12] K. Mal, I. Hussain, T. D. Memon, D. Kumar and B. S. Chowdhry, "Modern condition monitoring systems for railway wheel-set dynamics: Performance analysis and limitations of existing techniques," *Sir Syed University Research Journal of Engineering and Technology*, vol. 12, no. 1, pp. 31–41, 2022.
[13] S. Strano and M. Terzo, "Review on model-based methods for on-board condition monitoring in railway vehicle dynamics," *Advances in Mechanical Engineering*, vol. 11, no. 2, pp. 1–10, 2019.
[14] C. Li, S. Luo, C. Cole and M. Spiryagin, "An overview: Modern techniques for railway vehicle on board health monitoring systems," *Vehicle System Dynamics*, vol. 55, no. 7, pp. 1045–1070, 2017.
[15] J. Li, X. Qiu, Y. Wei, M. Song and X. Wang, "Online rail fastener detection based on YOLO network," *Computers, Materials and Continua*, vol. 72, no. 3, pp. 5955–5967, 2022.
[16] Y. Ma, P. Duan, P. He, F. Zhang and H. Chen, "FPGA implementation of extended kalman filter for SOC estimation of lithium-ion battery in electric vehicle," *Asian Journal of Control*, vol. 21, no. 4, pp. 2126–2136, 2019.
[17] B. Korotaj, B. Novoselnik and M. Baotic, "Kalman filter based sensor fusion for omnidirectional mechatronic system," in *2021 Int. Conf. on Electrical Drives & Power Electronics (EDPE)*, Dubrovnik, Croatia, pp. 183–188, 2021.
[18] L. F. Ávalos-Ruiz, C. J. Zúñiga-Aguilar, J. F. Gómez-Aguilar, R. F. Escobar-Jiménez and H. M. Romero-Ugalde, "FPGA implementation and control of chaotic systems involving the variable-order fractional operator with Mittag–Leffler law," *Chaos, Solitons and Fractals*, vol. 115, pp. 177–189, 2018.
[19] K. Mal, I. Hussain, B. Chowdhry and T. Memon, "Extended kalman filter for estimation of contact forces at wheel-rail interface," *3C TECNOLOGIA*, vol. 2020, no. Special Issue April 2020, pp. 279–301, 2020.
[20] K. Mal, I. Hussain, K. Shaikh, T. D. Memon, B. S. Chowdhry *et al.,* "A new estimation of nonlinear contact forces of railway vehicle," *Intelligent Automation and Soft Computing*, vol. 28, no. 3, pp. 823–841, 2021.
[21] T. Kumar, B. Pandey, T. Das and B. S. Chowdhry, "Mobile DDR Io standard based high performance energy efficient portable ALU design on FPGA," *Wireless Personal Communications*, vol. 76, no. 3, pp. 569–578, 2014.
[22] N. Instruments, "User guide and specifications NI myRIO-1900," *Datasheet*, vol. 2016, pp. 1–31, 2016.
[23] S. Munoz, J. Ros, P. Urda and J. L. Escalona, "Estimation of lateral track irregularity through kalman filtering techniques," *IEEE Access*, vol. 9, pp. 60010–60025, 2021.
[24] P. Hubbard, C. Ward, R. Dixon and R. Goodall, "Real time detection of low adhesion in the wheel/rail contact," *Proceedings of the Institution of Mechanical Engineers, Part F: Journal of Rail and Rapid Transit*, vol. 227, no. 6, pp. 623–634, 2013.
[25] M. Gokasan and C. Uyulan, "Extended kalman filter design for railway traction motor," *Selcuk University Journal of Engineering Science and Technolology*, vol. 5, no. 4, pp. 432–444, 2017.
[26] P. Goddard, "Goddard consulting (modeling. simulation. data analysis. visualization)," 2022. [Online]. Available: http://www.goddardconsulting.ca/simulink-extended-kalman-filter-quarter-car.html.
[27] K. Ishizaka, S. R. Lewis and R. Lewis, "The low adhesion problem due to leaf contamination in the wheel/rail contact: Bonding and low adhesion mechanisms," *Wear*, vol. 378–379, no. February 2017, pp. 183–197, 2017.
[28] I. Hussain, "Multiple model based real time estimation of wheel-rail contact conditions," Ph.D. Thesis, University of Salford MANCHESTER, 2012.